On the Origin of Regioselectivity in Palladium-Catalyzed Oxidation of Glucosides

Wan, Ieng Chim; Hamlin, Trevor A.; Eisink, Niek N.H.M.; Marinus, Nittert; de Boer, Casper; Vis, Christopher A.; Codée, Jeroen D. C.; Witte, Martin D.; Minnaard, Adriaan J.; Bickelhaupt, F. Matthias

Published in:
European Journal of Organic Chemistry

DOI:
10.1002/ejoc.202001453

Publication date:
2021

EurJOC
European Journal of Organic Chemistry

Communications
doi.org/10.1002/ejoc.202001453

Chemistry Europe
European Chemical Societies Publishing

On the Origin of Regioselectivity in Palladium-Catalyzed Oxidation of Glucosides

Ieng Chim (Steven) Wan,[a, b] Trevor A. Hamlin,[b] Niek N. H. M. Eisink,[a] Nittert Marinus,[a] Casper de Boer,[c] Christopher A. Vis,[c] Jeroen D. C. Codée,[c] Martin D. Witte,*[a] Adriaan J. Minnaard,*[a] and F. Matthias Bickelhaupt*[b, d]

The palladium-catalyzed oxidation of glucopyranosides has been investigated using relativistic density functional theory (DFT) at ZORA-BLYP–D3(BJ)/TZ2P. The complete Gibbs free energy profiles for the oxidation of secondary hydroxy groups at C2, C3, and C4 were computed for methyl β-glucoside and methyl carba-β-glucoside. Both computations and oxidation experiments on carba-glucosides demonstrate the crucial role of the ring oxygen in the C3 regioselectivity observed during the oxidation of glucosides. Analysis of the model systems for oxidized methyl β-glucoside shows that the C3 oxidation product is intrinsically favored in the presence of the ring oxygen. Subsequent energy decomposition analysis (EDA) and Hirschfeld charge analysis reveal the role of the ring oxygen: it positively polarizes C1/C5 by inductive effects and disfavors any subsequent buildup of positive charge at neighboring carbon atoms, rendering C3 the most favored site for the β-hydride elimination.

Carbohydrate chemistry remains a popular field of research due to its importance in biology. Like other important bio-molecules such as peptides, oligosaccharides are usually synthesized chemically using a bottom-up approach, starting with monosaccharide units and coupling them together via glycosylation.[1] This synthetic approach is highly adaptable for various oligosaccharides, but often contains numerous synthetic steps. This is because carbohydrates contain multiple hydroxy (OH) groups, which must first be selectively protected before glycosylation can occur in a regio- and stereoselective manner.[1,2] Site-selective (regioselective) reactions on (unprotected) carbohydrates are, therefore, highly desired and are often employed in the synthesis of functionalized carbohydrates. These reactions are well-developed to suit a variety of monosaccharides with different stereochemical configuration and with controllable selectivity for the desired transformation[3] and include, but are not limited to, acylation,[4,5] alkylation,[6] silylation,[7] and oxidation. While the utility of acylation, alkylation and silylation is clear in protecting-group chemistry, and acylation allows for limited subsequent modifications,[8] oxidation, on the other hand, allows further modifications such as epimerization, reductive amination, nucleophilic addition[9] and epoxidation[10] without further protection. One of the most well-studied oxidation reactions is the selective oxidation of pyranosides at C6 with TEMPO[11] or transition metal catalysts such as rhodium.[12] This makes use of the inherent lack of steric crowding of this primary hydroxy group. On the other hand, regioselective oxidation of the secondary hydroxy groups is far less common. Tin acetal mediated oxidation has been reported to induce high regioselectivity in glycosides containing cis-diols.[13] Our group reported on the catalytic C3-selective oxidation of glucopyranosides[14] using Waymouth's catalyst **2**[15] and has studied this reaction intensively (Scheme 1).

Since the discovery that glucosides can be oxidized selectively at the C3 position, this methodology has been used

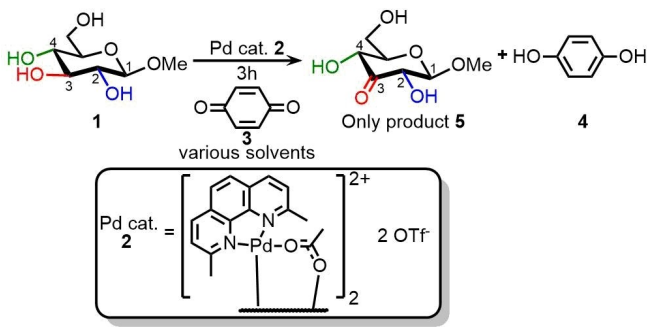

Scheme 1. C3-selective oxidation of methyl β-glucoside with Waymouth's catalyst.

[a] I. C. (Steven) Wan, Dr. N. N. H. M. Eisink, N. Marinus, Dr. M. D. Witte, Prof. Dr. A. J. Minnaard
Stratingh Institute for Chemistry,
University of Groningen
Nijenborgh 7, 9747 AG Groningen, The Netherlands
E-mail: m.d.witte@rug.nl
a.j.minnaard@rug.nl
[b] I. C. (Steven) Wan, Dr. T. A. Hamlin, Prof. F. M. Bickelhaupt
Department of Theoretical Chemistry
Amsterdam Institute of Molecular and Life Sciences (AIMMS),
Institution Amsterdam Center for Multiscale Modeling (ACMM),
Vrije Universiteit Amsterdam
De Boelelaan 1083, 1081 HV Amsterdam, The Netherlands
E-mail: f.m.bickelhaupt@vu.nl
[c] C. de Boer, C. A. Vis, Prof. Dr. J. D. C. Codée
Leiden Institute of Chemistry,
Leiden University
Einsteinweg 55, 2333 CC Leiden, The Netherlands
[d] Prof. F. M. Bickelhaupt
Institute for Molecules and Materials (IMM),
Radboud University
Heyendaalseweg 135, 6525 AJ Nijmegen, The Netherlands

Supporting information for this article is available on the WWW under https://doi.org/10.1002/ejoc.202001453

for the oxidation of various other monosaccharides and oligosaccharides.[16] In parallel, a number of studies have been carried out to investigate and challenge the C3-selectivity of the palladium catalyzed oxidation.[17a,b] The effect of the following factors on C3-selecitivity have been studied (Scheme 2): 1) steric crowding, 2) the stereochemical configuration and substitution pattern of the glycoside substrate, 3) the solvent, and 4) the temperature (Scheme 2). A competition experiment between **1** and its C4-THP protected variant showed that steric hindrance near C3 only results in decreased reactivity. However, it did not affect the site-selectivity.[17b] Varying substitution patterns on the glycoside do not alter the site-selectivity for C3 either.[14,17a,b] The apparent loss in regioselectivity in xylosides, galactosides and mannosides is the result of subsequent oxidation reactions on the keto-product, which leads to over-oxidation and rearrangement.[17b] Switching the solvent from a water/acetonitrile mixture to DMSO or trifluoroethanol affects the reaction rate, but in all cases the oxidation of the C3 OH is favored.[14,17a] Lastly, elevated reaction temperature erodes selectivity and results in the formation of the C4-oxidized product.[17a] Nevertheless, the C3 product dominates in all cases. Despite these mechanistic studies, the pertinent C3-selectivity has not been adequately explained. In this study, we show that the endocyclic oxygen is essential for the observed selectivity using a combination of synthetic experiments and computational chemistry.

We began our study by investigating the palladium-catalyzed oxidation of carba-β-glucose and carba-1-deoxyglucose, where the ring oxygen has been substituted by a methylene (CH_2) group. These substrates were synthesized (see Supporting Information for experimental methods and characterization) and subjected to oxidation conditions using catalyst **2**. Interestingly and in contrast to methyl β-glucoside, the oxidations of the carba-glucose derivatives were unselective and provided a nearly equal amount of C2, C3, and C4 oxidation products (and C1 oxidation in the case of carba-β-glucose) (Scheme 3). These experiments suggest that the ring oxygen plays a significant role in the regioselective C3 oxidation of methyl β-glucoside. To understand the influence of the ring oxygen on the regioselectivity, we next turn to density functional theory (DFT) calculations.

All calculations were carried out using the Amsterdam Density Functional (ADF) program[18] with dispersion-corrected relativistic density functional theory at ZORA-BLYP–D3(BJ)/TZ2P.[19] When noted, solvent effects of DMSO were modelled with COSMO.[20] Experimentally, it was observed that the use of solvents other than DMSO results in the same regioselectivity but with differing reaction rates.[14,17a] Throughout this paper, we focus on the electronic energies of the molecular systems. The Gibbs free energies at 298.15 K and 1 atm were calculated for the reactions as well, and trends in reactivity turned out to be unchanged. All open-shell systems were treated with the spin-unrestricted formalism at ZORA-(U)BLYP–D3(BJ)/TZ2P.

The reaction energies were computed for the oxidation of β-glucoside **1** with catalyst **2** in the presence of benzoquinone **3**, leading to all possible products and hydroquinone **4** (Scheme 4). Based on the experimental results and computations by Waymouth and coworkers,[15] we ruled out the possibility of oxidation at C6 and focused on the difference between the seemingly similar equatorial secondary alcohols at C2, C3, and C4. There are thus three possible outcomes of the oxidation: oxidation at C2, C3, C4, forming **5.2**, **5.3** and **5.4**, respectively. When the reaction was carried out at room

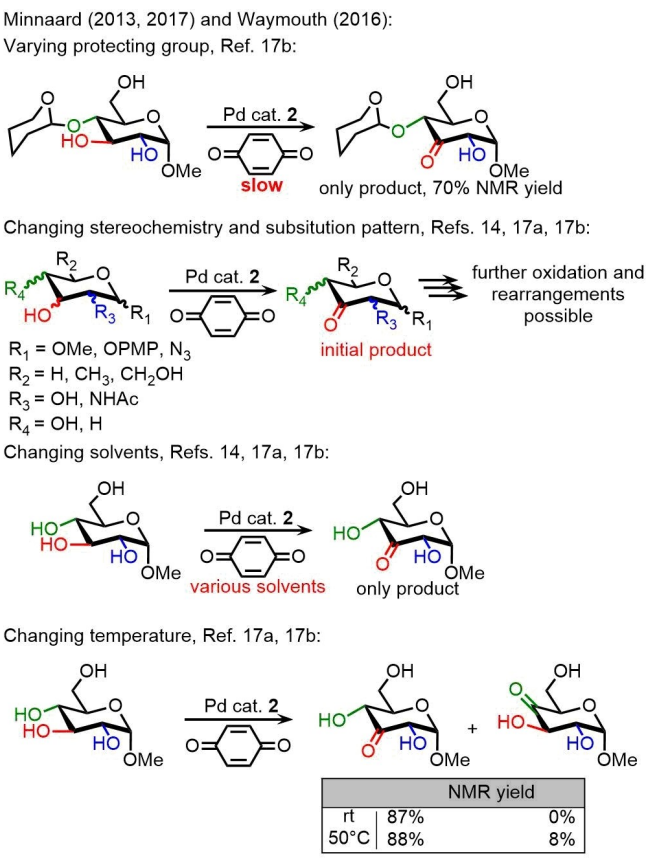

Scheme 2. Mechanistic studies carried out by our group and Waymouth and coworkers.

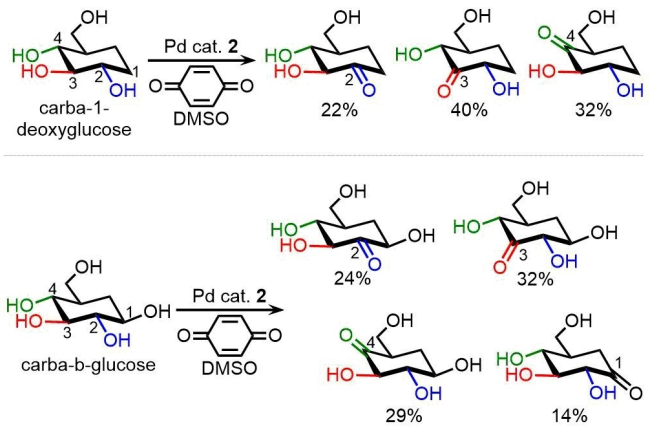

Scheme 3. Oxidation of carba-glucosides in DMSO using catalyst **2**. Only 1 eq benzoquinone was used. All yields are NMR yields.

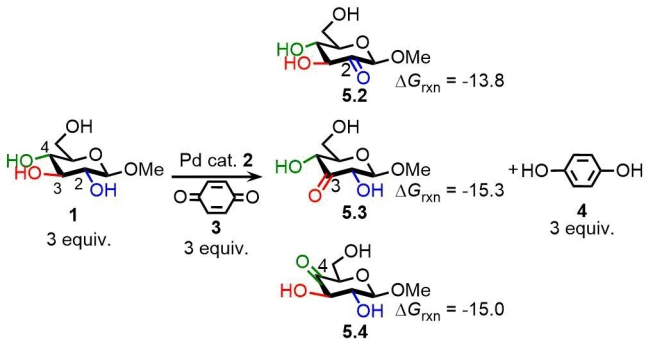

Scheme 4. Computed Gibbs free reaction energies (kcal mol^{-1}) for the formation of oxidized products **5.2**-**5.4** computed at COSMO(DMSO)-ZORA-BLYP–D3(BJ)/TZ2P.

temperature, product **5.3** was the observed product (Scheme 1). Our calculations found that formation of product **5.3** is the most exergonic reaction ($\triangle G_{rxn} = -15.3$ kcal mol^{-1}), followed by **5.4** ($\triangle G_{rxn} = -15.0$ kcal mol^{-1}), and then **5.2** ($\triangle G_{rxn} = -13.8$ kcal mol^{-1}). The small $\triangle\triangle G_{rxn}$ (0.3 kcal mol^{-1}) between **5.3** and **5.4** suggests that the formation of the experimentally observed **5.3** is under kinetic control, in line with the report of Waymouth[17a] whereby **5.4** was formed only when the reaction was heated.

The reaction mechanism proposed by Waymouth and co-workers[15] identifies the β-hydride elimination from a palladium-alkoxide species to a palladium-hydride species forming the carbonyl to be the rate determining step. The computed activation barriers and reaction energies for this step of the catalytic cycle associated with the formation of the oxidized products **5.2**, **5.3**, and **5.4** are provided in Table 1. The reaction begins with the reversible formation of hydroxyalkoxide reactant complexes **S2-4** (see Supplementary Information for detailed structures). The β-hydride elimination is initiated by the isomerization of **S** to the agostic alkoxide **S′**. A four-membered transition state was found for the β-hydride elimination **T** to form the corresponding palladium-hydride complex **U**. The energy differences between the different forms of **S** have little influence on the selectivity of the reaction, in line with the experimental observations; no significant rate difference was observed for the oxidation of glucoside **1**, 2-deoxyglucoside and 4-deoxyglucoside, despite the absence of a chelation equilibrium in the latter two substrates.[17b] The ~5 kcal mol^{-1} difference between the resting state **S** of C3 and C2/C4 could be attributed to the enhanced hydrogen bonding between the electron deficient Pd^{2+} bound O–H on C4 and O lone pair on C6, which does not exist in either the resting state **S** of C2 or C4. In the case of the resting state **S** of C2, a hydrogen bond is present between the O–H on C4 and O lone pair on C6, but it is very weak due to the fact that the acidity of the O–H proton on C4 is not enhanced by the coordination of O to Pd^{2+}. Structure **T** is the rate-determining transition state (TS) in all three pathways. The barrier of the C3-oxidation pathway has the lowest $\triangle E^{\ddagger}$ (12.7 kcal mol^{-1}). This $\triangle E^{\ddagger}$ is significantly lower than for C2/C4 oxidation ($\triangle\triangle E^{\ddagger}$ of 2.9 kcal mol^{-1} and 2.0 kcal mol^{-1}, respectively). The $\triangle G^{\ddagger}$ follows the same trend as the $\triangle E^{\ddagger}$. Calculations in DMSO (See Supplementary Information for details) show the same trend in selectivity ($\triangle G^{\ddagger}$: C3 < C4 < C2). In agreement with the previously reported experimental results, this indicates that solvation has little influence on the regioselectivity.[14,17a]

Table 1. Electronic energies ($\triangle E$) and [Gibbs free energies ($\triangle G$)] (in kcal mol^{-1}) of key intermediates and transition states in the β-hydride elimination of **1** and **1a** by the palladium-neocuproine complex relative to the most stable reactant complex **S3** computed at ZORA-BLYP–D3(BJ)/TZ2P. The C3 pathway is depicted below.

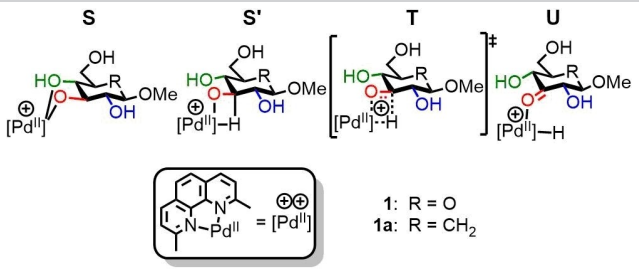

1 Pathway	**S**	**S′**	**T**	**U**
C2	5.3 [5.3]	9.4 [7.9]	15.6 [11.7]	9.3 [6.2]
C3	0.0 [0.0]	9.1 [7.2]	12.7 [9.1]	5.0 [1.9]
C4	5.3 [5.8]	11.5 [9.2]	14.7 [10.7]	9.7 [5.9]
1a Pathway	S	S′	T	U
C2	6.4 [6.8]	11.0 [8.9]	14.9 [11.6]	7.6 [6.0]
C3	0.0 [0.0]	10.2 [8.9]	13.8 [10.8]	5.0 [2.6]
C4	6.5 [5.9]	12.3 [10.5]	14.5 [11.1]	6.9 [3.7]

The electronic energies for the key structures of the mechanistic steps **S**→**S′**→**T**→**U** in the oxidation of carba-glucoside **1a** were also computed (Table 1). Carba-glucoside **1a** has the same molecular structure as β-glucoside **1**, except that the ring oxygen in **1** is replaced by a methylene (CH_2) group. In contrast to the results obtained for **1**, in the case of **1a** all three $\triangle E^{\ddagger}$ values are within 1.5 kcal mol^{-1}. Thus, the regioselectivity in the oxidation reaction disappears when moving from **1** to **1a**, in line with our experimental observations shown in Scheme 3.

From these results, it becomes clear that the ring oxygen has an influence on the regioselective oxidation of **1**. The correlation between the reactivity and the stability of the resulting oxidized products (**5.1**, **5.2**, and **5.3**) prompted us to next analyze model pyran systems **10a/b**, **11a/b**, **12a/b**, and **13a/b** (Scheme 5). These systems were judiciously selected with the aim to minimize any complicating features such as intramolecular hydrogen bonding and to allow for the underlying physics to be revealed. Furthermore, these model pyrans are ideal probes to establish the relationship between the carbonyl group that is formed during the reaction and the oxygen in the ring.

As we can see, each isoelectronic structure has a thermodynamic preference for the C3-keto structures (**10a**–**13a**) regardless of the substituents on the ring. Interestingly, the ring-opened structures (**14a/b**) again show a clear energetic preference for **14a**, the linear chain C3-keto analog of **10a**, over

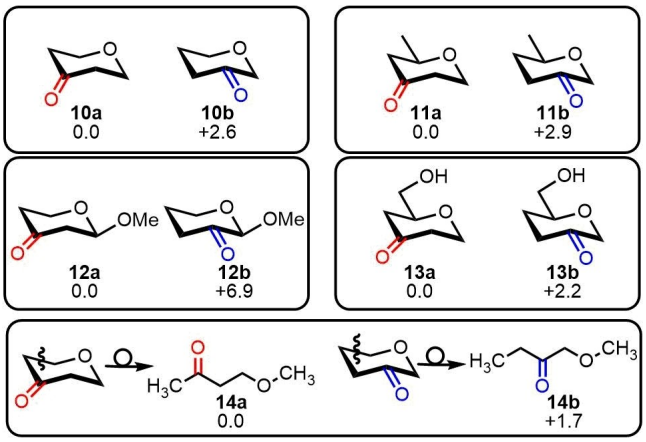

Scheme 5. Relative electronic energies ($\triangle E$, in kcal mol^{-1}) of isoelectronic C2- and C3-ketoglucosides analogs. Note that, in every case, the C3-ketoglucoside analogs (red) are more stable than the corresponding C2-ketoglucoside analogs (blue).

its regioisomer **14b**. From this, it can be concluded that the C3 preference retains in both cyclic and acyclic systems.

The results in Scheme 5 suggest that the effect of the ring oxygen is inductive, i.e., the ring oxygen disfavors proximal carbonyl groups (as in **10b**). In order to gain further insights into the relationship between the ring oxygen and the stability of the oxidized product, we focused our analysis on model systems **10a'** and **10b'** that have been optimized with a mirror plane (σ_h) in the C_{2v} and C_s point group, respectively. The bonding mechanism of the planar model systems **10a'** and **10b'** were analyzed using our energy decomposition analysis (EDA)[21] method. The EDA decomposes the $\triangle E_{int}$ between the two fragments **M** and **N** (Scheme 6a) into three physically meaningful energy terms: classical electrostatic interaction ($\triangle V_{elstat}$), steric (Pauli) repulsion ($\triangle E_{Pauli}$) which, in general, arises from two-center four-electron repulsions between the closed-shell orbitals of both fragments, and stabilizing orbital interactions ($\triangle E_{oi}$) that account for, among others, HOMO-LUMO interactions. The corresponding energy decomposition analysis (EDA) results are presented in Table 2.

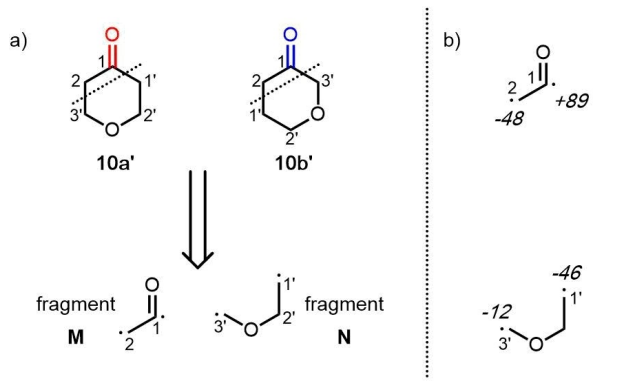

Scheme 6. a) EDA fragmentation scheme. **10a'** and **10b'** are artificially planar analogs of **10a** and **10b**, respectively and possess a mirror plane (σ_h). **10a'** and **10b'** were fully optimized and analyzed in C_{2v} and C_s symmetry, respectively. b) Hirschfeld charges (milli a.u.) of carbons with singly occupied orbitals on fragments **M** and **N**.

Since **10a'** and **10b'** are regioisomers comprised of the same molecular fragments **M** and **N**, the thermodynamic preference for **10a'** over **10b'** should be reflected in the $\triangle E_{int}$ between the two fragments. Indeed, we see that the $\triangle E_{int}$ slightly favors **10a'** over **10b'** (Table 2). By examining the contributions towards $\triangle E_{int}$, the electrostatic interaction $\triangle V_{elstat}$ is the most significant contributor for a favorable $\triangle E_{int}$ for **10a'**. To understand the trend in $\triangle V_{elstat}$, we analyzed the Hirschfeld charges of the terminal carbons of each fragment (Scheme 6b). Carbonyl carbon 1 on fragment **M** is the most positively polarized carbon in the fragment, while carbon 1' on fragment **N** is more negatively polarized compared to carbon 3'. The positively polarized carbonyl atom therefore interacts favorably with the (strongly) negatively polarized alkyl carbon during bond formation, which explains the thermodynamic preference for **10a'** over **10b'**. Generalizing this result, we argue that the build-up of positive charge is disfavored when the neighboring carbon is the α-carbon of the ring oxygen (in the case of compound **1**, C1 and C5, Scheme 7) Therefore, the oxidation is disfavored at C2/C4 relative to C3 because of the positive charge build-up during the formation of the carbonyl (i.e. β-hydride elimination).

In summary, we have computationally analyzed the mechanism of the C3 selective palladium-catalyzed oxidation reaction of methyl β-glucoside. Experimentally it was shown that the oxidation of methyl β-glucoside was regioselective for C3, whereas the same conditions for the oxidation of carba-β-glucoside (in which the ring oxygen is replaced with a meth-

Table 2. Energy decomposition analysis (in kcal mol^{-1}) of structures **10a'** and **10b'** computed at ZORA-(U)BLYP–D3(BJ)/TZ2P.

EDA term	**10a'**	**10b'**	Difference ($\triangle\triangle E_x$)[a]
$\triangle E_{int}$	−190.1	−189.9	−0.2
$\triangle V_{elstat}$	−288.7	−287.5	−1.2
$\triangle E_{Pauli}$	475.0	473.3	+1.7
$\triangle E_{oi}$	−370.5	−369.9	−0.6

[a] The difference is calculated as $\triangle\triangle E_x = \triangle E_x$ (**10a'**) − $\triangle E_x$ (**10b'**), where $\triangle E_x$ is the EDA term ($\triangle E_{int}$, $\triangle V_{elstat}$, $\triangle E_{Pauli}$, $\triangle E_{oi}$). A negative value for $\triangle\triangle E_x$ corresponds to an EDA term that favors the C3 oxidation product.

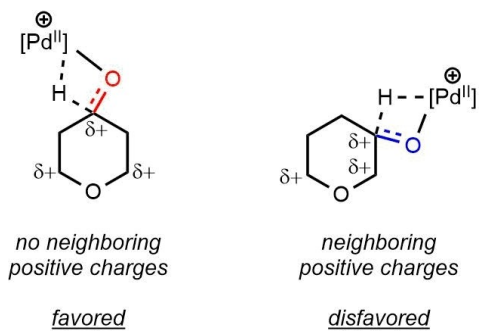

Scheme 7. Inductive effect of the ring oxygen on the selectivity of the β-hydride elimination.

ylene (CH_2) group) were unselective. These findings indicate that the ring oxygen plays a crucial role in the regioselective C3 oxidation. DFT studies verify that the β-hydride elimination of methyl β-glucoside at C3 has both the lowest activation barrier and is most exergonic compared to that at C2 or C4. These reactivity differences between C2, C3, and C4 vanish when the ring oxygen is removed in the case of carba-β-glucoside. Our bonding analyses on model methyl β-glucosides reveal that the predominant factor for the thermodynamic C3 preference originates from the unfavorable electrostatic interaction between the positively polarized α-carbon of the ring oxygen and the carbonyl carbon during β-hydride elimination. We envisage that the newly identified intramolecular electrostatic repulsion can serve as a general guideline for other molecules involving the creation of a ketone in a six-membered ring, in which an electronegative heteroatom is present.

Acknowledgements

We thank the Netherlands Organization for Scientific Research (NWO) for financial support.

Conflict of Interest

The authors declare no conflict of interest.

Keywords: Carbohydrates · Density functional calculations · Energy decomposition analysis · Oxidation · Regioselectivity

[1] a) A. E. Christina, L. J. van den Bos, H. S. Overkleeft, G. A. nan der Marel, J. D. C. Codée, *J. Org. Chem.* **2011**, *76*, 1692–1706; b) S. J. Danishefsky, Y.-K. Shue, M. N. Chang, C.-H. Wong, *Acc. Chem. Res.* **2015**, *48*, 643–652; c) P. Nagorny, B. Fasching, X. Li, G. Chen, B. Aussedat, S. J. Danishefsky, *J. Am. Chem. Soc.*, **2009**, *131*, 5792–5799.
[2] J. Guo, X.-S. Ye, *Molecules*, **2010**, *15*, 7235–7265.
[3] a) V. Dimakos, M. S. Taylor, *Chem. Rev.* **2018**, *118*, 11457–11517; b) M. Jäger, A. J. Minnaard, *Chem. Commun.* **2016**, *52*, 656–664.
[4] Y. Ueda, T. Kawabata in *Organocatalytic Site-Selective Acylation of Carbohydrates and Polyol Compounds, Topics in Current Chemistry, Vol. 372*, Springer International Publishing, **2016**, pp. 203–231.
[5] J. Lawandi, S. Rocheleau, N. Moitessier, *Tetrahedron*, **2016**, *72*, 6283–6319.
[6] T. Ogawa, M. Matsui, *Carbohydr. Res.* **1978**, *62*, C1–C4.
[7] R. S. Mancini, J. B. Lee, M. S. Taylor, *Org. Biomol. Chem.* **2017**, *15*, 132–143.
[8] a) M. Yanagi, Y. Ueda, R. Ninomiya, A. Imayoshi, T. Furuta, K. Mishiro, T. Kawabata, *Org. Lett.* **2019**, *21*, 5006–5009; b) S. W. Baldwin, S. A. Haut, *J. Org. Chem.* **1975**, *40*, 3885–3887.
[9] J. Zhang, N. N. H. M. Eisink, M. D. Witte, A. J. Minnaard, *J. Org. Chem.* **2019**, *84*, 516–525.
[10] N. Marinus, N. Tahiri, M. Duca, L. M. C. Marc Mouthaan, S. Bianca, M. van den Noort, B. Poolman, M. D. Witte, A. J. Minnaard, *Org. Lett.* **2020**, *22*, 5622–5626.
[11] M. T. C. Walvoort, D. Sail, G. A. van der Marel, J. D. C. Codée, in *Carbohydrate Chemistry: Proven Synthetic Methods, Vol. 1*, (Eds.: P. Kováč), CRC Press, **2016**, pp. 99–105.
[12] M. Trincado, K. Kühlein, H. Grützmacher, *Chem. Eur. J.* **2011**, *17*, 11905–11913.
[13] a) Y. Tsuda, M. Hanajima, N. Matsuhira, Y. Okuno, K. Kanemitsu, *Chem. Pharm. Bull. (Tokyo)* **1989**, *37*, 2344–2350; b) H.-M. Liu, Y. Sato, Y. Tsuda, *Chem. Pharm. Bull. (Tokyo)* **1993**, *41*, 491–501; c) W. Muramatsu, *Org. Lett.* **2014**, *16*, 4846–4849.
[14] M. Jäger, M. Hartmann, J. G. De Vries, A. J. Minnaard, *Angew. Chem. Int. Ed.* **2013**, *52*, 7809–7812; *Angew. Chem.* **2013**, *125*, 7963–7966.
[15] K. Chung, S. M. Banik, A. G. De Crisci, D. M. Pearson, T. R. Blake, J. V. Olsson, A. J. Ingram, R. N. Zare, R. N. Waymouth, *J. Am. Chem. Soc.* **2013**, *135*, 7593–7602.
[16] a) V. R. Jumde, N. N. H. M. Eisink, M. D. Witte, A. J. Minnaard, *J. Org. Chem.* **2016**, *81*, 11439–11443; b) N. N. H. M. Eisink, J. Lohse, M. D. Witte, A. J. Minnaard, *Org. Biomol. Chem.* **2016**, *14*, 4859–4864; c) J. Zhang, N. N. H. M. Eisink, Martin D. Witte, Adriaan J. Minnaard, *J. Org. Chem.* **2019**, *84*, 516–525.
[17] a) K. Chung, R. M. Waymouth, *ACS Catal.* **2016**, *6*, 4653–4659; b) N. N. H. M. Eisink, M. D. Witte, A. J. Minnaard, *ACS Catal.* **2017**, *7*, 1438–1445.
[18] a) G. Te Velde, F. M. Bickelhaupt, E. J. Baerends, C. Fonseca Guerra, S. J. A. van Gisbergen, J. G. Snijders, T. Ziegler, *J. Comput. Chem.* **2001**, *22*, 931–967; b) C. Fonseca Guerra, J. G. Snijders, G. Te Velde, E. J. Baerends, *Theor. Chem. Acc.* **1998**, *99*, 391–403; c) ADF2017.113, SCM Theoretical Chemistry, Vrije Universiteit: Amsterdam (Netherlands). http://www.scm.com.
[19] For ZORA: a) E. van Lenthe, E. J. Baerends, J. G. Snijders, *J. Chem. Phys.* **1993**, *99*, 4597–4610; b) E. van Lenthe, E. J. Baerends, J. G. Snijders, *J. Chem. Phys.* **1994**, *101*, 9783–9792; for BLYP:; c) A. D. Becke, *J. Chem. Phys.* **1986**, *84*, 4524; d) A. D. Becke, *Phys. Rev. A* **1988**, *38*, 3098–3100; for D3(BJ):; e) S. Grimme, J. Antony, S. Ehrlich, S. Krieg, *J. Chem. Phys.* **2010**, *132*, 154104; f) A. D. Becke, E. R. Johnson, *J. Chem. Phys.* **2005**, *123*, 154101; for TZ2P:; g) E. van Lenthe, E. J. Baerends, *J. Comput. Chem.* **2003**, *24*, 1142–1156.
[20] a) A. Klamt, G. Schüürmann, *J. Chem. Soc. Perkin Trans. 2* **1993**, 799–805; b) A. Klamt, *J. Phys. Chem.* **1995**, *99*, 2224–2235; c) A. Klamt, V. Jonas, *J. Chem. Phys.* **1996**, *105*, 9972–9981; d) C. C. Pye, T. Ziegler, *Theor. Chem. Acc.* **1999**, *101*, 396–408.
[21] a) F. M. Bickelhaupt, E. J. Baerends, in *Rev. Comput. Chem.* (Eds.: K. B. Lipkowitz, D. B. Boyd), Wiley, Hoboken, **2000**, pp. 1–86; b) R. van Meer, O. V. Gritsenko, E. J. Baerends, *J. Chem. Theory Comput.* **2014**, *10*, 4432–4441.

Manuscript received: November 5, 2020
Revised manuscript received: December 17, 2020
Accepted manuscript online: December 18, 2020